Enhancement of photoluminescence signal from ultrathin layers with silicon nanocrystals

S. A. Dyakov, D. M. Zhigunov, A. Hartel, M. Zacharias, T. S. Perova et al.

Citation: Appl. Phys. Lett. **100**, 061908 (2012); doi: 10.1063/1.3682537
View online: http://dx.doi.org/10.1063/1.3682537
View Table of Contents: http://apl.aip.org/resource/1/APPLAB/v100/i6
Published by the American Institute of Physics.

Enhancement of photoluminescence signal from ultrathin layers with silicon nanocrystals

S. A. Dyakov,[1] D. M. Zhigunov,[2] A. Hartel,[3] M. Zacharias,[3] T. S. Perova,[1,a)] and V. Yu. Timoshenko[2]
[1]*Department of Electronic and Electrical Engineering, Trinity College Dublin, Dublin 2, Ireland*
[2]*Faculty of Physics, M.V. Lomonosov Moscow State University, 119991 Moscow, Russia*
[3]*IMTEK, Faculty of Engineering, Albert-Ludwigs-University Freiburg, 79110 Freiburg, Germany*

(Received 21 December 2011; accepted 19 January 2012; published online 8 February 2012)

Using the model of oscillating dipoles, we simulated the photoluminescence intensity of a triple-layered structure where the silicon nanocrystals layer was enclosed by buffer and capping silicon dioxide layers. It was found that a structure with an optimized buffer layer thickness exhibited photoluminescence which was approximately 20 times more intense than that from the structure without a buffer layer. Theoretical simulations were verified by photoluminescence measurements for the corresponding structures with silicon nanocrystals fabricated by plasma enhanced chemical vapour deposition. © *2012 American Institute of Physics*. [doi:10.1063/1.3682537]

Ensembles of silicon nanocrystals (SiNCs) in silica matrix have been intensively studied over the last decades because of their ability to emit light at room temperature, to be compatible with standard silicon technology, and to have potential for optoelectronic applications.[1–3] The photoluminescence (PL) from structures with silicon nanocrystals can originate from the relaxation of highly localized defect states or from the band-to-band recombination of quantum confined excitons in the case of good passivation of defects.[1] Regardless of the origin of the PL, the emitted light can be out-coupled, re-absorbed by SiNCs or substrate, or coupled to waveguide modes.[4–6] The PL intensity of the sample strongly depends on the passive optical properties of the structure (i.e., spatial distribution of the refractive index) and the active optical properties of the emitting material (i.e., internal PL spectrum, position and orientation of point sources of PL).[5,7,8] Hence, the PL intensity from structures containing SiNCs can be significantly suppressed or enhanced by appropriate choice of the waveguiding properties.

An optical microcavity is a typical example of a structure which is used to enhance the light emission of a specific wavelength in a specific direction.[9] A SiNCs layer placed between two Bragg mirrors formed by silica layers exhibits a PL whose intensity is 100 times stronger than that of a simple SiNCs layer placed on top of a silicon wafer.[9] The PL intensity can also be strongly enhanced by proper coupling of the emitter field with surface plasmon polaritons (SPPs) supported by thin metal films.[10] This method requires a corrugated surface to compensate for the momentum mismatch between SPPs and emitted photons.

Another example where the spatial distribution of refractive index plays a crucial role in propagation of light is a layered structure with deposited anti-reflection coating. The significant decrease in the reflection coefficient of such structures is explained by the destructive interference of light reflected from the surfaces of the sample.[11] In the present study, we will apply this effect to the samples containing SiNCs for increasing the proportion of light which is emitted by the SiNCs and can emerge from the sample. The aim of the work is a calculation of the PL intensity from the triple-layered structures with SiNCs as a function of layer thicknesses as well as an experimental verification of the theoretical results.

The triple-layer thin films were fabricated on n-type (100)-Si substrates using an Oxford Instruments "Plasmalab 100" plasma enhanced chemical vapour deposition (PECVD) system with SiH_4 and N_2O as precursor gases. Variation of flow ratio $\Gamma = [N_2O]/[SiH_4]$ allows one to control the stoichiometry of the growing layers. Stoichiometric silicon dioxide (SiO_2) was deposited as a buffer and capping layer whereas silicon rich silicon oxynitride (SRON) was deposited as interlayer (see Fig. 1). The corresponding stoichiometry for the SRON layer was chosen to be $SiO_{1.0}N_{0.22}$. The composition of the layers was determined by x-ray photoelectron spectroscopy (XPS) with a PHI Quantum 2000 (Physical Electronics) XPS spectrometer. Subsequently, all samples were annealed for 1 h in a high purity N_2 atmosphere at 1150 °C in order to form SiNCs in the SRON layers. Further details on the sample preparation technique can be found elsewhere.[12] Thickness and refractive index of the films were measured using variable angle spectroscopic ellipsometry in an energy range of 1.1–4 eV at room temperature. Photoluminescence spectra were measured at room

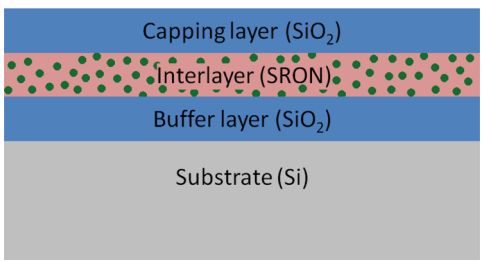

FIG. 1. (Color online) Schematic presentation of the investigated structures with silicon nanocrystals. SiNCs are shown by circles.

a)Author to whom correspondence should be addressed. Electronic mail: perovat@tcd.ie. Tel.: +353 1 896-14-32. Fax: +353 1 677-24-42.

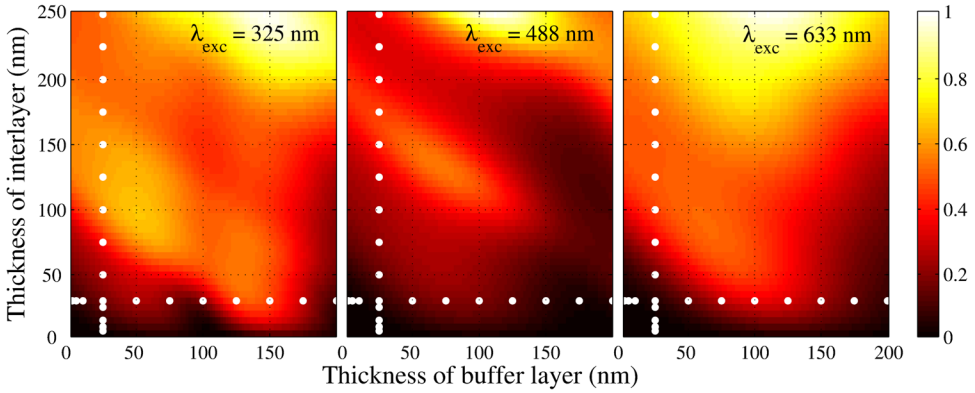

FIG. 2. (Color online) PL intensity as a function of interlayer and buffer layer thicknesses calculated using a model of oscillating dipoles. The white dots represent experimentally obtained data. The color scale on the right shows the calculated PL intensity.

temperature using a CCD camera attached to a single grating 500 mm focal length monochromator. HeCd (325 nm line), Ar^+ (488 nm line), and HeNe (633 nm line) lasers were used as excitation sources. All spectra were corrected for the spectral response of the optical setup.

The light emission by SiNCs is a quantum mechanical process with a random spatial emission of the respective photons, but the optical behavior of the emitted light can be modeled using classical electromagnetism.[4–8] In order to calculate the PL intensity from the samples containing the SiNCs, we use the optical model reported in Refs. 5 and 7. According to this model, one considers the ensemble of emitting SiNCs as a system of chaotically oriented oscillating electrical dipoles. The amplitude of oscillation of a dipole is proportional to the electric field strength of excitation light at the position of a dipole. The PL intensity from the SiNCs is approximated by the intensity of the outcoupled emission of such oscillating dipoles.

Each layer within the model structure is assumed to have smooth, parallel interfaces, and a certain thickness. The SRON interlayer is considered as a homogeneous isotropic layer with an effective dielectric permittivity $\tilde{\varepsilon}_2$. The emitting dipoles are located on planes which are uniformly distributed over this layer. The number of planes is proportional to the thickness of the interlayer. The propagation of the plane waves of excitation light and the plane waves emitted by oscillating dipoles is simulated by the transfer matrix method.[11] For the calculation, the dielectric permittivities of Si and SiO_2 are taken from the literature.[13] The values of the effective dielectric permittivity of the SRON layer at different wavelengths were determined by means of ellipsometry measurements. The values determined were $\tilde{\varepsilon}_2 = (2.11 + 0.15i)^2$ at 325 nm, $\tilde{\varepsilon}_2 = (1.88 + 0.019i)^2$ at 488 nm, $\tilde{\varepsilon}_2 = (1.84 + 0.007i)^2$ at 633 nm, and $\tilde{\varepsilon}_2 = (1.82 + 0.0025i)^2$ at 890, 930, and 940 nm. All PL intensities were calculated at normal angle of collection. The angles of incidence of the excitation light were 10° for 325 nm, 47° for 488 nm, and 39° for 633 nm. Laser beams were *s*-polarized for excitation wavelengths of 325 nm and 488 nm and *p*-polarized for 633 nm.

The PL intensity of a sample with SiNCs depends on three geometrical parameters, namely, the thicknesses of the capping, inter, and buffer layers, d_{cap}, d_{int} and d_{buf}, respectively. For the experimental verification of the theoretical results, two different sets of samples with SiNCs were fabricated. For the first set of samples, the thickness of the SiO_2 buffer layer was varied from 0 to 200 nm, while the thicknesses of interlayer and capping layer were fixed to 30 and 50 nm. On the contrary, the second set of samples was characterized by variable thickness of the SRON layer in the range from 10 to 250 nm, while the thicknesses of the SiO_2 layers were constant with 25 nm for the buffer and 50 nm for the capping layers.

In the first stage of simulation, the intensity of the light emitted by SiNCs, which emerges from the sample, was calculated for parameter d_{int} varying from 0 to 250 nm and d_{buf} varying from 0 to 200 nm. The calculations were performed for excitation wavelengths of $\lambda_{ex} = 325$ nm, 488 nm, and 633 nm and the corresponding emission wavelengths of $\lambda_{PL} = 890$ nm, 930 nm, and 940 nm in accordance with peak position of experimentally obtained PL spectra. The theoretically evaluated PL intensities are shown in Fig. 2 as a two-dimensional function of buffer and interlayer thicknesses. For excitation with $\lambda_{ex} = 325$ nm, the function has three local maxima in the investigated range of buffer layer and interlayer thicknesses. The local maximum at $d_{buf} = 50$ nm, $d_{int} = 100$ nm is the most interesting from the experimental point of view because the total sample thickness is the smallest. The simulated PL intensity curves for $\lambda_{ex} = 488$ nm and 633 nm have two local maxima and the most interesting ones are observed at $d_{buf} = 75$ nm, $d_{int} = 125$ nm for $\lambda_{ex} = 488$ nm, and $d_{buf} = 75$ nm, $d_{int} = 75$ nm for $\lambda_{ex} = 633$ nm. All the fabricated samples are denoted in Fig. 2 by white dots.

Experimentally obtained and calculated PL intensities for the first sets of samples are shown in Fig. 3 for $\lambda_{ex} = 325$ nm, 488 nm, and 633 nm. As can be seen from this figure, an excellent agreement was found between theoretical and experimental results. Note that the calculation method does not imply the use of any fitting parameters. In case of the 325 nm excitation wavelength, the function of PL intensity on d_{buf} has two local maxima in the investigated range (50 nm and 133 nm), and for 488 nm and 633 nm wavelengths, only one maximum exists at 75 nm and 100 nm, respectively. It is worth noting that the PL intensities from a structure with an optimized thickness of the buffer layer are about 20 times stronger than those obtained from the structures without a buffer layer.

From the optical point of view, the process of PL consists of two stages. The first stage is the in-coupling of the excitation wave into the structure with the SiNCs. All specific features of this stage, such as reflection and transmission coefficients, interference, and multireflection are determined by the excitation wavelength. The second stage

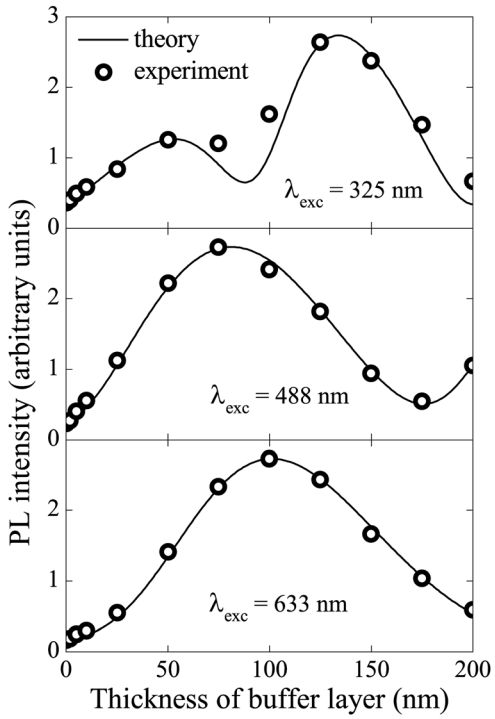

FIG. 3. Calculated (lines) and experimental (circles) PL intensities of the SiNCs samples as a function of the thickness of the buffer layer for different excitation wavelengths.

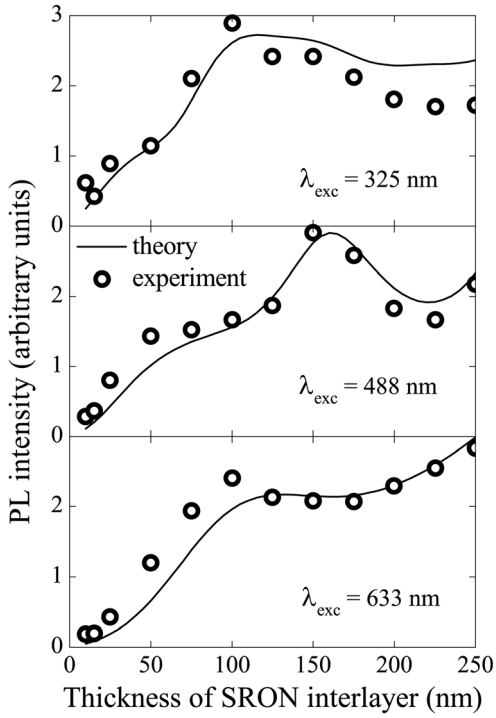

FIG. 5. Calculated (lines) and experimental (circles) PL intensities of the samples with SiNCs as a function of thickness of SRON interlayer at different excitation wavelengths.

is the emergence of the PL light from the sample. All characteristics of this stage are determined by the PL wavelength, i.e., by the size of the Si nanocrystals. In order to distinguish the contribution of the first stage on the resulting PL intensity, we calculated the average value of the square of the amplitude of the electric field strength over the SRON layer as a function of buffer layer thickness for $\lambda_{ex} = 325$ nm shown by dashed line in Fig. 4. For other excitation wavelengths, the results of calculations are similar. We will call this dependence as an in-coupling efficiency. Comparing the behavior of the PL intensity and the in-coupling efficiency, we can conclude that the distance between two peaks in the experimentally obtained dependence from Fig. 3 (at $\lambda_{ex} = 325$ nm) is mainly determined by the period of the function of in-coupling efficiency. Further, we calculated the PL intensity

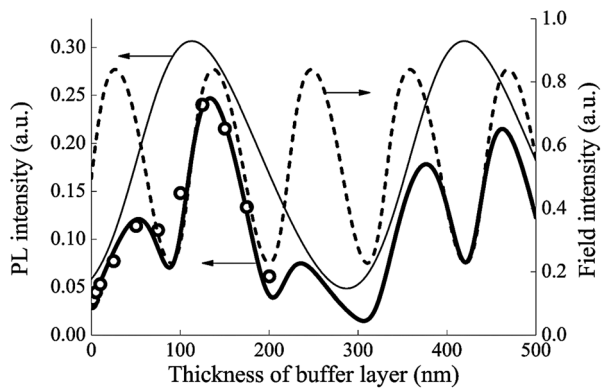

FIG. 4. Comparison of in-coupling (dashed line) and out-coupling (thin solid line) efficiencies with calculated (thick solid line) and experimental (dots) PL intensities of the SiNCs samples as functions of buffer layer thickness.

for the specific case when the amplitude of oscillation of the dipole is constant and does not depend on the excitation electric field strength (thin solid line in Fig. 4). In fact, a calculated PL intensity for this case is an out-coupling efficiency. This approach enables us to distinguish the contribution of the second stage, the emerging PL light from the sample. As can be seen in Fig. 4, the function of the out-coupling efficiency is the envelope curve to the experimentally verified dependence of the PL intensity as a function of the buffer layer thickness. Thus, the ratio between the amplitude of the peaks in the experimental dependence (see Fig. 3 at $\lambda_{ex} = 325$ nm) is mainly determined by the period of the function of out-coupling efficiency. This period as well as the period of the function of in-coupling efficiency can be found from the condition for the two nearest Fabry-Pérot resonances which appear during the propagation of excitation or PL light through the buffer layer:[11] $\Delta d_{buf} = \frac{\lambda}{2n_3 \cos f}$, where λ is the wavelength of excitation or PL light, n_3 is the refractive index of buffer layer and f is the angle of light propagation in the buffer layer.

The experimental and calculated PL intensities for the second series of samples with variable SRON layer thickness are shown in Fig. 5. It can be seen that dependencies of the PL intensity are neither a linear or monotonically increasing functions of the thickness of the interlayer, but have local maxima and minima. The position of local maxima is $d_{buf} = 100$ nm for the excitation wavelengths $\lambda_{ex} = 325$ nm and 633 nm, and $d_{buf} = 150$ nm for $\lambda_{ex} = 488$ nm. This result is quite unexpected, since the number of SiNCs in the sample is proportional to the thickness of SRON layer and, at first sight, the PL intensity should also increase monotonically as a function of the SRON interlayer thickness. It is obvious now that such a statement is untrue, and it is possible, for

example, to obtain more intense luminescence from a thinner emitting layer but enclosed with optimized buffer and/or capping layers. Note, that the agreement between calculated curves and experimental data plotted in Fig. 5 is not as good as for the set of samples with different buffer layer thickness. This is most likely caused by thickness dependent changes in the SiNCs ensemble (e.g., SiNCs size distribution) which were not taken into account by our simple model.[14] As in case of series 1, the features of the dependencies of PL intensity on the thickness of interlayer can be explained by Fabry-Pérot resonances for both excitation and PL lights.

In conclusion, we performed a quantitative analysis of the processes of excitation of PL light and its subsequent emergence from the SiNCs containing sample. It was found that the PL intensity of the investigated samples is strongly influenced by the Fabry-Pérot resonances appearing during the propagation of excitation and PL light through the sample. The enhancement of the photoluminescence intensity by a factor of 20 can be observed for a structure with optimized buffer layer thickness compared to non-optimized one. Theoretically predicted PL intensities are in very good agreement with results of the photoluminescence measurements for the corresponding structures with silicon nanocrystals.

S.D. acknowledges Irish Research Council for Science, Engineering and Technology (IRCSET) and Trinity College Dublin for financial support. D.Z. and M.Z. acknowledge financial support from German Research Foundation (ZA191/27–1).

[1]S. Godefroo, M. Hayne, M. Jivanescu, A. Stesmans, M. Zacharias, O. I. Lebedev, G. Van Tendeloo, and V. V. Moshchalkov, Nat. Nanotechnol. **3**, 174 (2008).
[2]L. Pavesi, L. Dal Negro, C. Mazzoleni, G. Franzo, and F. Priolo, Nature **408**, 440 (2000).
[3]R. J. Walters, G. I. Bourianoff, and H. A. Atwater, Nature Mater. **4**, 143 (2005).
[4]R. J. Walters, J. Kalkman, A. Polman, H. A. Atwater, and M. J. A. de Dood, Phys. Rev. B **73**, 132302 (2006).
[5]K. A. Neyts, J. Opt. Soc. Am. A **15**, 962 (1998).
[6]R. Meerheim, M. Furno, S. Hofmann, B. Lüssem, and K. Leo, Appl. Phys. Lett. **97**, 253305 (2010).
[7]H. Benisty, R. Stanley, and M. Mayer, J. Opt. Soc. Am. A **15**, 1192 (1998).
[8]C. E. Reed, J. Giergiel, J. C. Hemminger, and S. Ushioda, Phys. Rev. B **36**, 4990 (1987).
[9]F. Iacona, G. Franzò, E. C. Moreira, and F. Priolo, J. Appl. Phys. **89**, 8354 (2001).
[10]E. Takeda, T. Nakamura, M. Fujii, S. Miura, and S. Hayashi, Appl. Phys. Lett. **89**, 101907 (2006).
[11]P. Markoš and C. M. Soukoulis, *Wave Propagation: From Electrons to Photonic Crystals and Left-Handed Materials* (Princeton University Press, Princeton, NJ, 2008).
[12]A. M. Hartel, D. Hiller, S. Gutsch, P. Löper, S. Estradé, F. Peiró, B. Garrido, and M. Zacharias, Thin Solid Films **520**, 121 (2011).
[13]E. D. Palik and G. Ghosh, *Handbook of Optical Constants of Solids*, Vol. 3 (Academic, New York, 1998).
[14]Y. C. Fang, W. Q. Li, L. J. Qi, L. Y. Li, Y. Y. Zhao, Z. J. Zhang, and M. Lu, Nanotechnology **15**, 494 (2004).